JOURNAL OF BACTERIOLOGY, July 1990, p. 3842–3848
0021-9193/90/073842-07$02.00/0

Vol. 172, No. 7

Cloning, Sequence, and Expression of the Pantothenate Permease (*panF*) Gene of *Escherichia coli*

SUZANNE JACKOWSKI[1]* AND JEAN-HERVE ALIX[2]

Departments of Biochemistry, St. Jude Children's Research Hospital and University of Tennessee, Memphis, Tennessee 38101,[1] and Institut de Biologie Physico-Chimique, and University of Paris 7, 13 rue Pierre et Marie Curie, 75005 Paris, France[2]

Received 6 December 1989/Accepted 9 April 1990

Pantothenate permease, the product of the *panF* gene, catalyzes the sodium-dependent uptake of extracellular pantothenate. The *panF* gene was isolated from an *Escherichia coli* genomic DNA library and subcloned into multicopy plasmids. Increased copy number of the *panF*$^+$ allele resulted in increased rates of pantothenate uptake and a significant increase in the steady-state intracellular pantothenate concentration. Despite the higher levels of pantothenate, the utilization of pantothenate for coenzyme A formation was not elevated, indicating that pantothenate kinase activity is the dominant regulator of coenzyme A biosynthesis. DNA sequencing of the *panF* gene revealed the presence of a single open reading frame that encoded a hydrophobic protein with a molecular weight of 51,992. Sequence analysis predicts that pantothenate permease is an integral membrane protein possessing 12 hydrophobic membrane-spanning domains connected by short hydrophilic sequences. The predicted topological profile of pantothenate permease is similar to that of other membrane carriers that catalyze cation-dependent symport.

Coenzyme A (CoA) is the predominant acyl group carrier in living systems. Nearly 100 enzymes require CoA (1), and this cofactor also modulates the activity of several key enzymes of intermediary metabolism (for reviews, see references 1, 6, and 17), suggesting that control over the intracellular CoA concentration is an important aspect of metabolic regulation. CoA is formed by a universal series of reactions beginning with the phosphorylation of the vitamin pantothenic acid (1). *Escherichia coli* produces its own abundant supply of this vitamin (9) from the condensation of β-alanine and pantoic acid (3). The level of intracellular CoA is modulated by control over pantothenate phosphorylation and by the degradation of CoA and acyl carrier protein (ACP) to 4'-phosphopantetheine (20, 21). Physiological, biochemical, and genetic evidence points to feedback inhibition of pantothenate kinase primarily by CoA and secondarily by CoA thioesters as a key regulated step in the biosynthetic pathway (20, 21). Pantothenate, the kinase substrate, is derived from either de novo biosynthesis from β-alanine or by uptake from the extracellular medium. The intracellular pantothenate pool is small (<1 μM [9, 22]), and excess endogenous pantothenate is efficiently effluxed from the cell (9, 22). These observations suggest that the maintenance of low substrate levels may be required for optimal kinetic control of pantothenate phosphorylation. The rate of pantothenate uptake from the medium is determined by the activity of pantothenate permease (22), the product of the *panF* gene (23). The pantothenate carrier is an inner membrane protein that concentrates the vitamin by a sodium cotransport mechanism (22). Although the transport system has a high affinity for pantothenate, the maximum velocity is 100-fold less than that of typical amino acid transport processes, indicating that the permease is not an abundant protein (22).

The goal of the present work was to evaluate the role of the pantothenate transport system by cloning the permease structural gene and overproducing the carrier in vivo to determine whether elevated uptake activity increases the steady-state intracellular concentration of pantothenate and subsequently elevates the level of cellular CoA.

MATERIALS AND METHODS

Chemicals and supplies. Sources for supplies were: Amersham Corp., L-[^{35}S]methionine (specific activity, 1,174 Ci/mmol), ACS scintillation solution, and ^{14}C-methylated protein standards; Analabs Inc., 250-μm Silica Gel H plates; Boehringer Mannheim Biochemicals, restriction endonucleases, T4 DNA ligase, and yeast tRNA; Difco Laboratories, BiTek agar, Bacto-tryptone, and Bacto-yeast extract; Du Pont NEN Research Products, β-[3-^{3}H]alanine (specific activity, 120 Ci/mmol), D-[1-^{14}C]pantothenic acid (specific activity, 55 Ci/mol), and En^{3}Hance; FMC Corp., SeaKem agarose; Pharmacia P-L Biochemicals, ATP; Research Organics, Inc., dithiothreitol; Sigma Chemical Co., β-alanine, D-pantothenate, lysozyme, and amino acids. All other chemicals were reagent grade or better.

Bacterial strains and plasmids. All strains used in this study were derivatives of *E. coli* K-12 and are listed in Table 1. Strains defective in pantothenate permease (*panF11*) did not exhibit a mutant growth phenotype in the absence of a Pan$^-$ background, which was provided by the presence of the *panD2* mutation. For the physiological experiments, an isogenic series of strains were constructed starting with strain C600 (Table 1). The *panD2* (9), *panF11* (23), *coaA14*(Ts) (20), and *recA1* alleles were sequentially introduced into strain C600 by P1 phage-mediated transduction by using closely linked transposon Tn*10* elements for selection. Cells were grown in minimal medium E (24) supplemented with glucose (0.4%), leucine (0.01%), threonine (0.01%), and either β-alanine (4 μM) or pantothenate (4 μM) unless otherwise indicated. Antibiotics were as follows: ampicillin, 50 μg/ml; chloramphenicol, 40 μg/ml; and tetracycline hydrochloride, 10 μg/ml. Cell number was determined with a Klett-Summerson colorimeter with a blue filter calibrated for strain C600 or strain SJ148, a *recA1* derivative of strain C600. The number of viable bacteria was deter-

* Corresponding author.

TABLE 1. Bacterial strains used in this study

Strain	Relevant genotype	Construction or source
C600	*thr-1 leuB6 lacY1 thi-1 supE44 tonA21* λ⁻ F⁻	B. Bachman (CGSC)[a]
DV49	*gltA fabE22*(Ts) *panD2 panF11 lct mtl xyl ara tsx galK thi lacY zhc-9*::Tn*10* (λ)	P1(DV11) × DV44 (21)
MB1986	*fabE22*(Ts) *zhc-46*::Tn*10 prmA3* λ⁻	2
SJ148	*thr-1 leuB6 lacY1 thi-1 supE44 tonA21 recA1 zfi*::Tn*10* λ⁻ F⁻	This study
SJ177	*thr-1 leuB6 lacY1 thi-1 supE44 tonA21 panD2 coaA14*(Ts) *recA*::Tn*10* (cml) λ⁻ F⁻	This study
SJ180	*thr-1 leuB6 lacY1 thi-1 supE44 tonA21 panD2 panF11 recA1 zfi*::Tn*10* λ⁻ F⁻	This study
SJ207	*thr-1 leuB6 lacY1 thi-1 supE44 tonA21 panD2 recA1 zfi*::Tn*10* λ⁻ F⁻	This study

[a] CGSC, *E. coli* Genetic Stock Center, Yale University, New Haven, Conn.

mined by plating samples from growing cultures, and these values were plotted as a function of the colorimeter readings.

Pantothenate transport assays. Pantothenate uptake assays were performed and initial rates were determined as described previously (22) with 20 μM extracellular [1-^{14}C]pantothenate. Initial transport rates were determined by calculating the slope of the uptake with 15-s time points within the first minute of the assay. Initial rates were expressed as picomoles per minute per 10^8 cells. Cell numbers were measured for each transport experiment by determining the number of CFU per milliliter immediately before chloramphenicol was added. Rates were calculated from duplicate determinations made on two separate occasions. Intracellular volume was assumed to be 0.437 μl per 5×10^6 cells or, equivalently, 2.5 μl/mg (dry weight) (18).

Metabolic labeling experiments. Strains SJ207 and SJ207(pSJ2) were grown in minimal medium E containing glucose (0.4%), leucine (0.01%), threonine (0.01%), and [1-^{14}C]pantothenate (25 μM). Cells were harvested in the late logarithmic stage of growth at a density of 10^9 cells per ml. The cells were separated from the medium by centrifugation, and the labeled metabolites were extracted as described previously (9). Cell extracts were treated with dithiothreitol to convert thioesters and disulfides to free sulfhydryl forms and analyzed by thin-layer chromatography on Silica Gel H layers developed with either ethanol–28% ammonium hydroxide (4:1) or butanol-acetic acid-water (5:2:4) to 14 cm above the origin. The distribution of radioactivity on the chromatogram was determined by using a Bioscan Imaging Detector.

Cloning of the *panF* gene. An *E. coli* genomic library was kindly provided by J. Lupski. The library was constructed by the partial digestion of chromosomal DNA with *Sau*3AI and ligation of these fragments into the *Bam*HI cloning sites in λ phage Charon 28 (12). Lysogens of recombinant plus wild-type helper phages were then selected at 42°C after infection of strain MB1986 [*fabE22*(Ts)] as described previously (2). A total of 75 thermoresistant lysogens were identified, and λ phage lysates were prepared by UV light induction. Recombinant phage plaques were purified and tested again for the correction of the *fabE22*(Ts) mutation. The isolated λ (*fabE22*$^+$) transducing phages were then used to infect strain DV49 [*panD2 panF11 fabE22*(Ts)]. A total of 58 of the 75 transductants that grew at 42°C also exhibited the Pan$^+$ growth phenotype, indicating that they carried the *panF* gene. One of these phages, λFA6, that contained both the *panF* and *fabE* genes was chosen for subcloning and sequencing (2). Overlapping segments of both strands were subcloned into M13 mp18 and mp19 and sequenced with the Applied Biosystems Automated Sequencer operated by the St. Jude Molecular Resource Center. The *panF* sequence was submitted to the Genetic Sequence Data Bank (GenBank) and was assigned accession number M30953.

RESULTS

Isolation of the *panF* gene. First, recombinant λ transducing phages were isolated that corrected both the *fabE22*(Ts) and *panF11* growth phenotypes (see Materials and Methods). One of these phages (λFA6) was selected for further study, and the 16-kilobase (kb) chromosomal insert was cleaved with *Bam*HI into three fragments of 6, 5.5, and 4.4 kb. Each of these was subcloned into the *Bam*HI site of pBR322, and strain DV49 was transformed with the recombinant plasmids. Transformants were selected for ampicillin resistance and tested for correction of the *panF11* and *fabE22*(Ts) growth phenotypes. Both phenotypes were complemented by the 6-kb *Bam*HI fragment, and the plasmid carrying this insert was designated pFA (2). With this plasmid (Fig. 1), a restriction enzyme map of the chromosomal insert was prepared, and the DNA fragments were subcloned into pBR322 to prepare a series of plasmids with different portions of the original 6-kb insert. These plasmids were transformed into strain SJ180 (*panF11 panD2*) and scored for their ability to grow on pantothenate or β-alanine (Fig. 1). These experiments localized the *panF* gene within the 1.5-kb fragment between the *Bam*HI and *Eco*RV sites of plasmid pFD5 (Fig. 1).

The initial rates of pantothenate transport were determined in strain SJ180 (*panF*) harboring each of these recombinant plasmids (Table 2). The wild-type (single-copy) rate of pantothenate uptake was 0.4 pmol/min per 10^8 cells in strain SJ207, whereas pantothenate uptake was not detected in strain SJ180 (*panF*). In strain SJ180 harboring either the pFA, pSJ2, or pFE2, the initial rate of pantothenate accumulation averaged 5.9 pmol/min per 10^8 cells, a 10-fold increase in permease activity. Interestingly, the pFD5 plasmid was able to correct the growth phenotype of strain SJ180 on pantothenate (Fig. 1); however, the initial rate of pantothenate transport in strain SJ180 containing plasmid pFD5 was the same as the wild-type transport rate (Table 2). Since there was no difference in the recovery of plasmid DNA from these strains, this result suggested that pFD5 did not contain the complete pantothenate permease gene and/or regulatory elements.

Elevated pantothenate transport activity results in higher intracellular concentrations of pantothenate. We determined whether enhanced uptake activity was associated with a significant increase in the steady-state intracellular concentration of pantothenate (Fig. 2). For this experiment, we used strain SJ177 [*coaA*(Ts)], which had a temperature-sensitive pantothenate kinase activity, blocking the phosphorylation and further metabolism of pantothenate at the nonpermissive temperature (42°C). Cells were grown to mid-logarithmic phase at 30°C in medium containing 1 μM pantothenate to minimize the intracellular pantothenate pool before the transport measurement was made. The cells were then washed free of pantothenate and incubated at 42°C for 20 min in medium without pantothenate to ensure complete

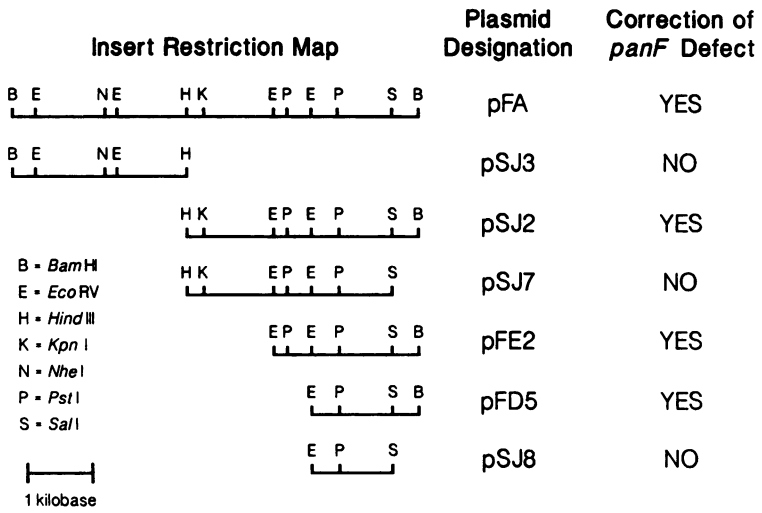

FIG. 1. Restriction endonuclease maps of inserts into pBR322. The location of restriction enzyme cleavage sites, plasmid designations, and the ability of the plasmids to correct the *panF* growth phenotype when transformed into strain SJ180 are indicated. In all cases the fragments shown were subcloned into the corresponding unique restriction sites in plasmid pBR322. The insert present in plasmid pFA was the 6.0-kb *Bam*HI fragment obtained from the digestion of the original recombinant λFA6 phage that corrected both the *panF* and the *fabE22*(Ts) phenotypes. Plasmids pSJ2 and pSJ3 are the same as plasmids pFH and pFI, respectively (2).

depletion of the normally undetectable intracellular pool and to inactivate the kinase. Transport measurements were made during the initial uptake period and continued until the uptake rate decreased to zero, representing the equilibration of influx and efflux rates. Strain SJ177 possessed wild-type pantothenate permease activity at 42°C (0.5 pmol/min per 10^8 cells) and accumulated pantothenate to an estimated intracellular concentration of 20 μM in the presence of 1 μM extracellular pantothenate at 42°C (Fig. 2). In contrast, strain SJ177(pSJ2) accumulated pantothenate to a constant concentration of approximately 85 μM at 42°C. These data illustrate that the pantothenate pool was not strictly regulated and that the pantothenate efflux system did not effectively compete with increased pantothenate uptake activity, resulting in an elevated intracellular pantothenate concentration in strains that overexpressed the permease.

Interrelationships between pantothenate transport activity and CoA content. We examined whether the intracellular CoA level had an effect on the rate of pantothenate uptake, both in the wild-type strain SJ177 and in strain SJ177(pSJ2), which overexpresses the permease protein and exhibits at least a 10-fold-higher pantothenate transport rate. Strain SJ177 contained the *panD2* and *coaA14*(Ts) defects. These mutations allowed regulation of the intracellular CoA level by varying the amount of input β-alanine (9) and the segregation of transport from further metabolism of the vitamin by eliminating pantothenate phosphorylation at the nonpermissive temperature (21). Cells were grown at 30°C to midlogarithmic phase in either 1 or 100 μM β-alanine, yielding intracellular CoA levels of 6 and 40 pmol/10^8 cells, respectively. The cells were harvested and washed, and the pantothenate uptake activity was measured at 42°C and at 30°C. At 30°C, strain SJ177 demonstrated an average transport rate of 0.14 pmol/min per 10^8 cells at the high CoA level and 0.4 pmol/min per 10^8 cells at the low CoA concentration. The influence of CoA on pantothenate uptake was similar in strain SJ177(pSJ2) assayed at 30°C: 3.84 pmol/min per 10^8 cells after growth on 1 μM β-alanine and 8.2 pmol/min per 10^8 cells following growth on 100 μM β-alanine. These results could be interpreted as an effect of CoA on pantoth-

TABLE 2. Pantothenate transport activity in strain SJ180 (*panF*) harboring recombinant plasmids[a]

Strain	Transport activity (pmol/min per 10^8 cells)
SJ207 (*pan*$^+$)	0.4
SJ180 (*panF*)	0.0
SJ180(pBR322)	0.0
SJ180(pFA)	5.5
SJ180(pSJ2)	6.1
SJ180(pSJ3)	0.0
SJ180(pFD5)	0.4
SJ180(pFE2)	6.2

[a] Initial rates were calculated from pantothenate transport assays performed with 10 μM extracellular pantothenate as described in Materials and Methods.

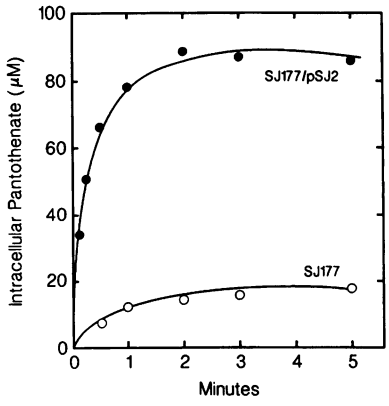

FIG. 2. Accumulation of intracellular pantothenate in a strain that overexpresses pantothenate transport activity. The pantothenate content per 10^8 cells was determined by using the standard pantothenate transport method with 1 μM extracellular [^{14}C]pantothenate as described in Materials and Methods. Intracellular pantothenate concentrations were estimated by assuming a cell volume 0.437 μl per 5×10^8 cells (18).

TABLE 3. Levels of pantothenate-derived metabolites in strains SJ207 and SJ207(pSJ2) grown in the presence of 25 μM extracellular pantothenate[a]

Metabolite	Concn (pmol/10^8 cells)	
	SJ207	SJ207(pSJ2)
CoA	30.4	34.6
ACP	5.1	6.0
Pantothenate	ND[b]	2.3

[a] Strains were grown on glucose minimal medium containing [1-^{14}C]pantothenate to a density of 10^9 cells per ml. Cells were harvested and extracted, and the distribution of label among the intracellular metabolites was determined by thin-layer chromatography as described in Materials and Methods.
[b] ND, Not detected.

enate transport, but might instead reflect the influence of CoA on the pantothenate kinase activity and the rate of pantothenate incorporation into CoA.

To test this point, transport assays were also performed at 42°C. There was no significant difference between the initial rates of transport at 42°C at either high or low intracellular CoA levels. Strain SJ177 had a rate that averaged 0.8 pmol/min per 10^8 cells and strains SJ177(pSJ2) averaged 9.6 pmol/min per 10^8 cells under both CoA conditions. Thus, in the absence of pantothenate incorporation into CoA and further metabolism, the initial pantothenate transport rate was unaffected by the intracellular CoA concentration.

We next determined whether transmembrane pantothenate flux played a role in the overall regulation of CoA production by measuring the effect of a larger pantothenate pool on the production of CoA. Strains SJ207 and SJ207(pSJ2) were grown in the presence of 25 μM D-[1-^{14}C]pantothenate (specific activity, 55 Ci/mol) to cell densities of 3×10^8, 4.5×10^8 and 8×10^8 cells per ml, and the cells were harvested. The amount of each pantothenate-derived metabolite in the cultures was determined by thin-layer chromatography and scintillation counting (Table 3). Strain SJ207 (*panD2*) and its derivatives were used because this strain was not able to synthesize pantothenate due to a defect in aspartate-1-decarboxylase. In strain SJ207, the CoA content was 30.4 pmol/10^8 cells, and intracellular pantothenate was not present in detectable quantities. Although strain SJ207(pSJ2) had a significant intracellular pantothenate pool (2.3 pmol/10^8 cells; 26 μM), the cellular CoA content was not appreciably different from that in the isogenic strain that did not harbor the pSJ2 plasmid. The ACP level was also not affected by the presence of a large intracellular pantothenate pool. Thus, regulation of CoA

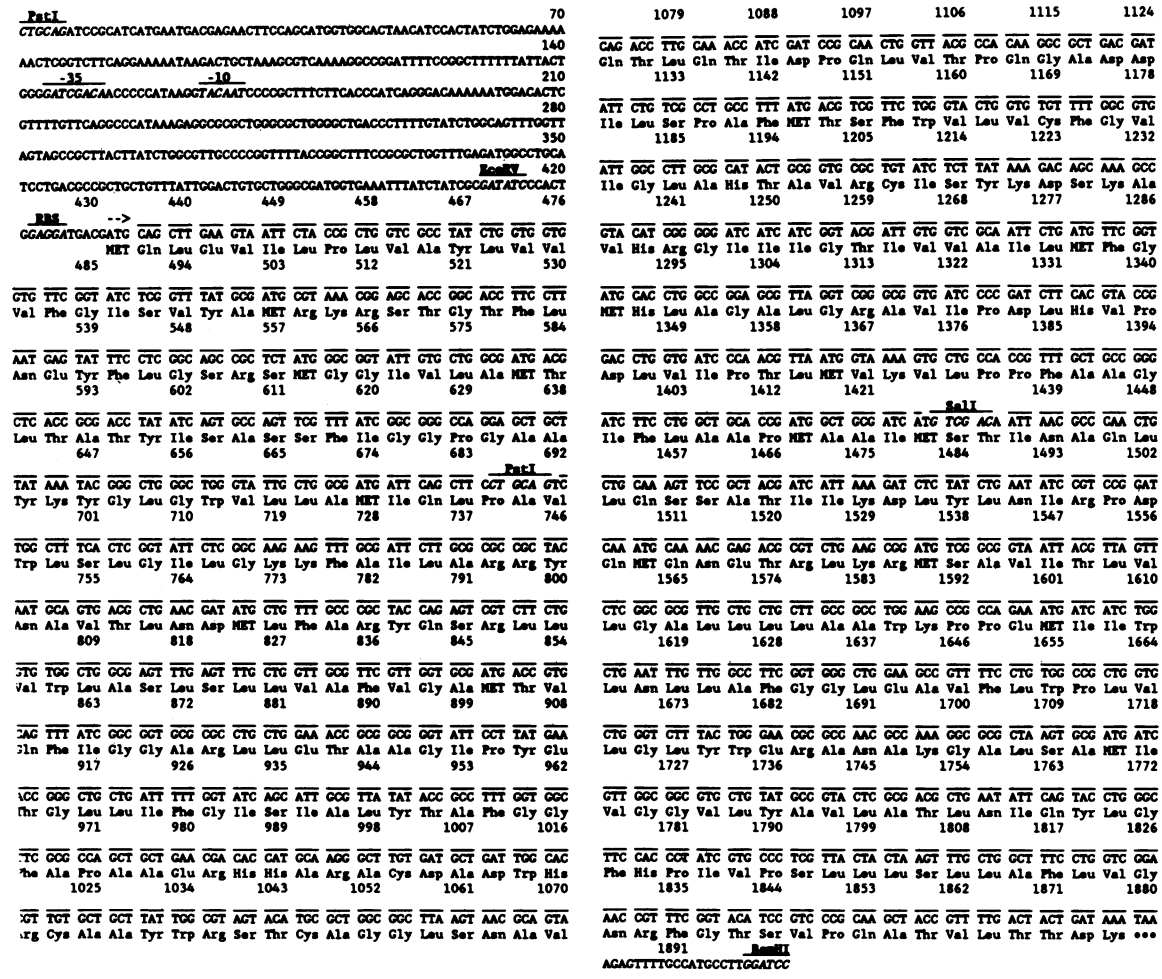

FIG. 3. Nucleotide sequence and predicted amino acid sequence of *panF*. Numbering of the DNA sequence starts from the 5′ end at the *Pst*I site and proceeds to the *Bam*HI site. The −35 and −10 promoter regions and the Shine-Dalgarno ribosome-binding sequence (RBS) are boxed. The three dots under the TAA at position 1876 indicate the termination codon. Relevant restriction endonuclease sites are indicated.

TABLE 4. Predicted amino acid composition of pantothenate permease[a]

Amino acid	No. of residues	% of total
Nonpolar		
Leu	74	15.3
Ala	62	12.7
Gly	41	8.5
Val	39	8.1
Ile	36	7.5
Phe	22	4.6
Pro	21	4.4
Met	17	3.5
Tyr	16	3.3
Trp	10	2.1
Cys	5	1.0
Total	343	71.2
Polar		
Thr	27	5.6
Ser	26	5.4
Arg	20	4.1
Gln	14	2.9
Lys	12	2.5
Asp	12	2.5
Asn	11	2.3
Glu	9	1.9
His	8	1.7
Total	139	28.8

[a] Summarized from data in Fig. 3.

biosynthesis at the pantothenate kinase step is the most important determinant of pantothenate utilization. Increased intracellular pantothenate had no influence on CoA content, indicating that efflux of the vitamin did not have a regulatory role in the scheme of CoA biosynthesis.

Nucleotide sequence of the *panF* gene. The region between the *Bam*HI site and the distal *Pst*I site was selected for subcloning into M13 and sequenced (Fig. 3). The 1,904 base pairs (bp) that were sequenced contained a single open reading frame beginning at position 432 and ending at 1880 with a TAA stop codon. At 6 bp upstream of the ATG start site was the GAGGA consensus sequence for ribosome binding (Shine-Dalgarno sequence). A second ATG start site was located 6 bp upstream of the ATG initiation site at 432 (Fig. 3); however, this ATG constituted part of the GAGGA ribosome-binding site, suggesting that translation is initiated at the downstream ATG at position 432. A sequence corresponding to the Pribnow box (TACAAT) was located at

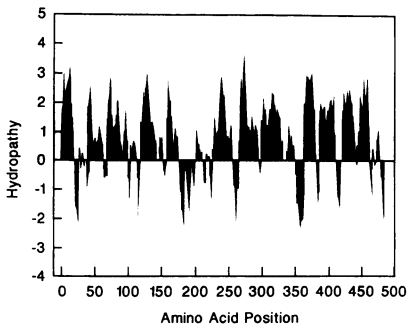

FIG. 4. Hydropathy profile of pantothenate permease. Hydropathy was calculated by the method of Kyte and Doolittle (11) with a span of six residues. The portions of the protein sequence above the midpoint line indicate predicted hydrophobic regions, and the portions below the line indicate predicted hydrophilic regions.

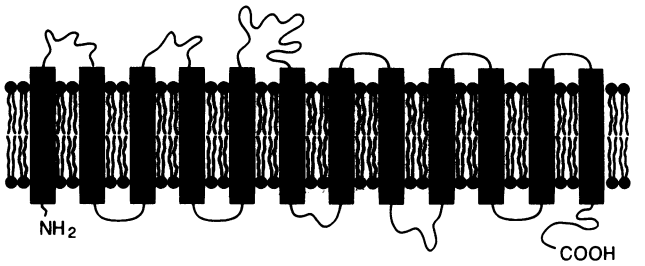

FIG. 5. Topological model of pantothenate permease. Pantothenate permease is predicted to consist of 12 hydrophobic transmembrane domains (shown as rectangles) connected by short hydrophilic domains.

position 164, with a −35 sequence (GATCGACAA) located at 144. Although these regions exhibited a high degree of homology with consensus *E. coli* promoter motifs, additional experiments will be required to confirm the promoter activity of these sequences. No information on the *panF* terminator located downstream of the *Bam*HI site is available because this region was not cloned into the original λFA6 (Fig. 1).

Plasmid pFD5 was capable or correcting the *panF* growth defect (Fig. 1) but did not overproduce pantothenate permease transport activity (Table 2). The *Eco*RV-*Bam*HI fragment contains the entire coding sequence for pantothenate permease, but the promoter elements have been removed (Fig. 3). Since only low levels of pantothenate transport activity are required to supply pantothenate for CoA biosynthesis, diminished *panF* expression due to removal of the promoter elements accounts for the correction of the *panF* growth phenotype and for the low rate of pantothenate transport activity exhibited by strains transformed with plasmid pFD5.

Deduced amino acid sequence of pantothenate permease. The amino acid sequence of pantothenate permease predicted from the nucleotide sequence is presented in Fig. 3. The sequence predicts a protein product of M_r 51,922, consisting of 482 amino acid residues that begins at the ATG found at 432 and terminates at the TAA codon located at 1878 (Fig. 3). The permease contained a very high proportion (71.2%) of hydrophobic amino acids (Table 4). Leucine was the most abundant amino acid (74 of 482 residues). Pantothenate permease was predicted to be a basic protein because it contains 21 acidic amino acid residues and 32 basic residues, giving an excess of 11 positive charges at neutral pH. The frequency of optimal codon usage calculated by the method of Ikemura (8) was 0.64. This value was consistent with the low abundance of pantothenate permease (22) and was similar to those of other *E. coli* permeases, such as *lacY* (0.62), *putP* (0.66), and *melB* (0.57).

The hydropathy (hydrophilicity and hydrophobicity) of the pantothenate carrier was calculated along the amino acid sequence by the method of Kyte and Doolittle (11) with a six-residue span (Fig. 4). The pantothenate permease contained 12 predicted hydrophobic segments flanked by short hydrophilic regions. Like *melB* (25), *lacY* (4, 7), and *putP* (16), the *panF* sequence (Fig. 3) did not have the hallmarks of a signal sequence at the amino-terminal end, suggesting that, like other bacterial carriers, the *panF* gene product was not synthesized in a precursor form. The 12 hydrophobic segments had a mean length of 23.6 residues, which is characteristic of the membrane-spanning, α-helical domains found in integral membrane proteins such as the lactose carrier (7). Foster et al. (7) reported that the length of a

24-residue α-helical peptide is about 3.6 nm, corresponding to the thickness of the hydrophobic core of the membrane. Kyte and Doolittle (11) suggest that if the average hydropathy of a given 19-residue span is greater than +1.6, there is a high probability that it composes a membrane-spanning region of the molecule. In pantothenate permease, 11 of the 12 proposed transmembrane domains had average hydropathies greater than +1.6. The second hydrophobic region in the protein had an average value of +1.4, which is higher than that for proposed membrane-spanning domains of other bacterial permeases (7, 16). The longest hydrophilic stretch of amino acids occurred between membrane-spanning segments 5 and 6. Whether this hydrophilic loop is intracellular or exposed to the periplasmic space is unknown. Therefore, analysis of the predicted amino acid sequence of pantothenate permease suggests that it is an integral membrane protein with 12 hydophobic, transmembrane α-helical motifs (Fig. 5).

DISCUSSION

Analysis of the *panF* sequence reveals that pantothenate permease has a predicted structure that places it in the same category as other integral membrane cation-dependent symport systems. A topological model for pantothenate permease based on the hydropathy profile of the predicted amino acid sequence is shown in Fig. 5. The permease has 12 membrane-spanning hydrophobic regions separated by short hydrophilic segments. This topological motif is found in other cation-dependent membrane carriers. This list includes the *putP* (16), *lacY* (4, 7), *melB* (25), *xylE* (13), and *araE* (14) genes of *E. coli*, the yeast *GAL2* (19) and *SNF3* (5) hexose carriers, the murine anion-exchange protein (10), and the human glucose transporter (15). Despite the similarity in amino acid composition and the strong topological resemblance of *panF* to other carriers, the protein or nucleic acid sequence of *panF* does not contain regions that are significantly homologous to any of these transporters. This includes the *putP* (16), *lacY* (4, 7), *melB* (25), *xylE* (13), and *araE* (14) genes of *E. coli*. In contrast, bacterial, yeast, and mammalian hexose transport systems do have areas of sequence homology (19), suggesting a common origin for these genes distinct from *panF*.

Our physiological experiments argue against a significant role for pantothenate permease in the regulation of CoA content. Cells harboring hybrid plasmids containing the *panF* gene showed significantly increased rates of pantothenate uptake (Table 2) and had higher intracellular concentrations of pantothenate (Fig. 2, Table 3). However, this dramatic increase in the supply of the vitamin did not translate into increased amounts of CoA (Table 3). These data clearly point to the phosphorylation of pantothenate by pantothenate kinase as the key regulated step in controlling the flux of pantothenate through the CoA-biosynthetic pathway. This conclusion is consistent with other biochemical and genetic evidence suggesting that feedback regulation of pantothenate kinase by CoA and its thioesters is a major determinant of CoA levels in *E. coli*. Whereas pantothenate permease functions to accumulate the extracellular vitamin, alterations in the activity of this transport system do not influence the pattern of pantothenate utilization.

ACKNOWLEDGMENTS

We thank Pamela Jackson for her excellent technical assistance. We also thank Clayton Naeve and the St. Jude Molecular Resource Center for DNA sequencing. Our appreciation is extended to Barabara Bachmann for supplying strains of *E. coli* K-12 from the Coli Genetic Stock Center. We also acknowledge Marianne Grunberg-Manago, in whose laboratory part of this work was done, for her continued interest and James R. Lupski for the lambda library.

This work was supported by Public Health Service grant GM-34496 from the National Institutes of Health, grants-in-aid from the American Heart Association (851165 and 880664), Cancer Center (CORE) support grant CA-21865, and the American Lebanese and Syrian Associated Charities. This work was also supported by the Centre National de la Recherche Scientifique (grant to URA 1139) and the Ministère des Affaires Étrangeres (Direction de la Cooperation Scientifique et Technique), which donated the travel funds to J.H.A.

LITERATURE CITED

1. **Abiko, Y.** 1975. Metabolism of coenzyme A, p. 1–25. *In* D. M. Greenburg (ed.), Metabolic pathways, vol. 7, 3rd ed. Academic Press, Inc., New York.
2. **Alix, J. H.** 1989. A rapid procedure for cloning genes from lambda libraries by complementation of *E. coli* defective mutants: application to the *fabE* region of the *E. coli* chromosome. DNA **8**:779–789.
3. **Brown, G. M.** 1959. The metabolism of pantothenic acid. J. Biol. Chem. **249**:7747–7755.
4. **Buchel, D. E., B. Gronenborn, and B. Muller-Hill.** 1980. Sequence of the lactose permease gene. Nature (London) **283**: 541–545.
5. **Celenza, J. L., L. Marshal-Carlson, and M. Carlson.** 1988. The SNF3 gene encodes a glucose transporter homologous to the mammalian protein. Proc. Natl. Acad. Sci. USA **85**:2130–2134.
6. **Dawes, E. A., and P. J. Large.** 1982. Class I reactions: supply of carbon skeletons, p. 125–158. *In* J. Mandelstam, K. McQuillen, and I. Dawes (ed.), Biochemistry of bacterial growth. John Wiley & Sons, Inc., New York.
7. **Foster, D. L., M. Boublik, and H. R. Kabak.** 1982. The structure of the *lac* carrier protein of *Escherichia coli*. Biochemistry **21**:5800–5805.
8. **Ikemura, T.** 1981. Correlation between the abundance of *Escherichia coli* transfer RNAs and the occurrence of the respective codons in its protein genes: a proposal for a synonymous codon choice that is optimal for the *E. coli* translational system. J. Mol. Biol. **151**:389–409.
9. **Jackowski, S., and C. O. Rock.** 1981. Regulation of coenzyme A biosynthesis. J. Bacteriol. **148**:926–932.
10. **Kopito, R. R., and H. F. Lodish.** 1985. Primary structure and transmembrane orientation of the murine anion exchange protein. Nature (London) **316**:234–238.
11. **Kyte, J., and R. F. Doolittle.** 1982. A simple method for displaying the hydrophobic character of a protein. J. Mol. Biol. **157**:105–132.
12. **Lupski, J. R., B. L. Smiley, F. R. Blattner, and G. N. Godson.** 1982. Cloning and characterization of the *Escherichia coli* chromosomal region surrounding the *dnaG* gene, with a correlated physical and genetic map of *dnaG* generated via transposon Tn*5* mutagenesis. Mol. Gen. Genet. **185**:120–128.
13. **Maiden, M. C. J., E. O. Davis, S. A. Baldwin, D. C. M. Moore, and P. J. F. Henderson.** 1987. Mammalian and bacterial sugar transporters are homologous. Nature (London) **325**:641–643.
14. **Maiden, M. C. J., M. C. Jones-Mortimer, and P. J. F. Henderson.** 1988. The cloning, DNA sequence, and overexpression of the gene *araE* coding for arabinose-proton symport in *Escherichia coli* K12. J. Biol. Chem. **263**:8003–8010.
15. **Mueckler, M., C. Caruso, S. A. Baldwin, M. Panico, I. Blench, H. R. Morris, W. J. Allard, G. E. Lienhard, and H. F. Lodish.** 1985. Sequence and structure of a human glucose transporter. Science **229**:941–945.
16. **Nakao, T., I. Yamato, and Y. Anraku.** 1987. Nucleotide sequence of *putP*, the proline carrier gene of *Escherichia coli* K12. Mol. Gen. Genet. **208**:70–75.
17. **Robishaw, J. D., and J. R. Neely.** 1985. Coenzyme A metabolism. Am. J. Physiol. **248**:E1–E9.
18. **Stock, J. B., B. Rauch, and S. Roseman.** 1977. Periplasmic space

in *Salmonella typhimurium* and *Escherichia coli*. J. Biol. Chem. **252**:7850–7861.
19. **Szkutnicka, K., J. F. Tschopp, L. Andrews, and V. P. Cirillo.** 1989. Sequence and structure of the yeast galactose transporter. J. Bacteriol. **171**:4486–4493.
20. **Vallari, D. S., and S. Jackowski.** 1988. Biosynthesis and degradation both contribute to the regulation of coenzyme A content in *Escherichia coli*. J. Bacteriol. **170**:3961–3966.
21. **Vallari, D. S., S. Jackowski, and C. O. Rock.** 1987. Regulation of pantothenate kinase by coenzyme A and its thioesters. J. Biol. Chem. **262**:2468–2471.
22. **Vallari, D. S., and C. O. Rock.** 1985. Pantothenate transport in *Escherichia coli*. J. Bacteriol. **162**:1156–1161.
23. **Vallari, D. S., and C. O. Rock.** 1985. Isolation and characterization of *Escherichia coli* pantothenate permease (*panF*) mutants. J. Bacteriol. **164**:136–142.
24. **Vogel, H. J., and D. M. Bonner.** 1956. Acetylornithinase of *Escherichia coli*: partial purification and some properties. J. Biol. Chem. **218**:97–106.
25. **Yazyu, H., S. Shiota-Niiya, T. Shimamoto, H. Kanazawa, M. Futai, and T. Tsuchiya.** 1984. Nucleotide sequence of the *melB* gene and the characteristics of the deduced amino acid sequence of the melibiose carrier in *Escherichia coli*. J. Biol. Chem. **259**:4320–4326.